

000  
 001  
 002  
 003  
 004  
 005  
 006  
 007  
 008  TURNING THE SPELL AROUND: LIGHTWEIGHT  
 009 ALIGNMENT AMPLIFICATION VIA RANK-ONE SAFETY  
 010 INJECTION  
 011  
 012  
 013

008 **Anonymous authors**

009 Paper under double-blind review

012 ABSTRACT  
 013

014 Safety alignment in Large Language Models (LLMs) often involves mediating  
 015 internal representations to refuse harmful requests. Recent research has demon-  
 016 strated that these safety mechanisms can be bypassed by ablating or removing  
 017 specific representational directions within the model. In this paper, we propose  
 018 the opposite approach: RANK-ONE SAFETY INJECTION (ROSI), a white-box  
 019 method that *amplifies* a model’s safety alignment by permanently steering its ac-  
 020 tivations toward the refusal-mediating subspace. ROSI operates as a simple, fine-  
 021 tuning-free rank-one weight modification applied to all residual stream write ma-  
 022 trices. The required safety direction can be computed from a small set of harmful  
 023 and harmless instruction pairs. We show that ROSI consistently increases safety  
 024 refusal rates - as evaluated by LLAMA GUARD 3 - while preserving the utility  
 025 of the model on standard benchmarks such as MMLU, HELLASWAG, and ARC.  
 026 Furthermore, we show that ROSI can also re-align ‘uncensored’ models by am-  
 027 plifying their own latent safety directions, demonstrating its utility as an effective  
 028 last-mile safety procedure. Our results suggest that targeted, interpretable weight  
 029 steering is a cheap and potent mechanism to improve LLM safety, complementing  
 030 more resource-intensive fine-tuning paradigms.

031 *Warning: This document may contain harmful or unsafe prompts.*

032  
 033 1 INTRODUCTION  
 034

035 Large language models (LLMs) have demonstrated striking generality (Brown et al., 2020), ex-  
 036 ceelling across tasks ranging from factual question answering (Kamalloo et al., 2023) and reasoning  
 037 (Wei et al., 2023b) to code synthesis (Tong & Zhang, 2024) and creative writing (Gómez-Rodríguez  
 038 & Williams, 2023). Their versatility has made them the foundation of modern conversational as-  
 039 sistant and productivity tools, where alignment techniques such as supervised fine-tuning and rein-  
 040 forcement learning from human feedback enable models to follow user instructions while adhering  
 041 to safety constraints (Ouyang et al., 2022). As general-purpose interfaces for language interaction,  
 042 LLMs are now widely deployed, fueling expectations that they may one day serve as core compo-  
 043 nents of autonomous, high-stakes systems.

044 Yet the same properties that make LLMs powerful also render them fragile and exposed to attack.  
 045 Pre-training on vast, uncurated corpora inevitably imbues models with the capacity to generate harm-  
 046 ful content (Wu et al., 2024), and safety alignment through post-training optimization offers only  
 047 a partial safeguard (Mendu et al., 2025). Researchers have shown that even carefully aligned chat  
 048 models remain vulnerable to a growing arsenal of jailbreak strategies, including prompt injection,  
 049 obfuscation, multilingual exploits, and fine-tuning aimed at suppressing refusal, all capable of cir-  
 050 cumventing safety guardrails (Lin et al., 2024; Chu et al., 2024; Wei et al., 2023a).

051 Recent advances in mechanistic interpretability shed light on why these vulnerabilities arise. In  
 052 particular, Ardit et al. (2024) demonstrate that refusal behavior is mediated by a *one-dimensional*  
 053 *linear direction* in the activation space of many open-source chat models. Erasing this “refusal di-  
 054 rection” from the residual stream suffices to disable safety alignment, enabling harmful comple-  
 055 tions;

054  
 055  
 056  
 057  
 058  
 059  
 060  
 061  
 062  
 063  
 064  
 065  
 066  
 067  
 068  
 069  
 070  
 071  
 072  
 073  
 074  
 075  
 076  
 077  
 078  
 079  
 080  
 081  
 082  
 083  
 084  
 085  
 086  
 087  
 088  
 089  
 090  
 091  
 092  
 093  
 094  
 095  
 096  
 097  
 098  
 099  
 100  
 101  
 102  
 103  
 104  
 105  
 106  
 107  
 108  
 109  
 110  
 111  
 112  
 113  
 114  
 115  
 116  
 117  
 118  
 119  
 120  
 121  
 122  
 123  
 124  
 125  
 126  
 127  
 128  
 129  
 130  
 131  
 132  
 133  
 134  
 135  
 136  
 137  
 138  
 139  
 140  
 141  
 142  
 143  
 144  
 145  
 146  
 147  
 148  
 149  
 150  
 151  
 152  
 153  
 154  
 155  
 156  
 157  
 158  
 159  
 160  
 161  
 162  
 163  
 164  
 165  
 166  
 167  
 168  
 169  
 170  
 171  
 172  
 173  
 174  
 175  
 176  
 177  
 178  
 179  
 180  
 181  
 182  
 183  
 184  
 185  
 186  
 187  
 188  
 189  
 190  
 191  
 192  
 193  
 194  
 195  
 196  
 197  
 198  
 199  
 200  
 201  
 202  
 203  
 204  
 205  
 206  
 207  
 208  
 209  
 210  
 211  
 212  
 213  
 214  
 215  
 216  
 217  
 218  
 219  
 220  
 221  
 222  
 223  
 224  
 225  
 226  
 227  
 228  
 229  
 230  
 231  
 232  
 233  
 234  
 235  
 236  
 237  
 238  
 239  
 240  
 241  
 242  
 243  
 244  
 245  
 246  
 247  
 248  
 249  
 250  
 251  
 252  
 253  
 254  
 255  
 256  
 257  
 258  
 259  
 260  
 261  
 262  
 263  
 264  
 265  
 266  
 267  
 268  
 269  
 270  
 271  
 272  
 273  
 274  
 275  
 276  
 277  
 278  
 279  
 280  
 281  
 282  
 283  
 284  
 285  
 286  
 287  
 288  
 289  
 290  
 291  
 292  
 293  
 294  
 295  
 296  
 297  
 298  
 299  
 300  
 301  
 302  
 303  
 304  
 305  
 306  
 307  
 308  
 309  
 310  
 311  
 312  
 313  
 314  
 315  
 316  
 317  
 318  
 319  
 320  
 321  
 322  
 323  
 324  
 325  
 326  
 327  
 328  
 329  
 330  
 331  
 332  
 333  
 334  
 335  
 336  
 337  
 338  
 339  
 340  
 341  
 342  
 343  
 344  
 345  
 346  
 347  
 348  
 349  
 350  
 351  
 352  
 353  
 354  
 355  
 356  
 357  
 358  
 359  
 360  
 361  
 362  
 363  
 364  
 365  
 366  
 367  
 368  
 369  
 370  
 371  
 372  
 373  
 374  
 375  
 376  
 377  
 378  
 379  
 380  
 381  
 382  
 383  
 384  
 385  
 386  
 387  
 388  
 389  
 390  
 391  
 392  
 393  
 394  
 395  
 396  
 397  
 398  
 399  
 400  
 401  
 402  
 403  
 404  
 405  
 406  
 407  
 408  
 409  
 410  
 411  
 412  
 413  
 414  
 415  
 416  
 417  
 418  
 419  
 420  
 421  
 422  
 423  
 424  
 425  
 426  
 427  
 428  
 429  
 430  
 431  
 432  
 433  
 434  
 435  
 436  
 437  
 438  
 439  
 440  
 441  
 442  
 443  
 444  
 445  
 446  
 447  
 448  
 449  
 450  
 451  
 452  
 453  
 454  
 455  
 456  
 457  
 458  
 459  
 460  
 461  
 462  
 463  
 464  
 465  
 466  
 467  
 468  
 469  
 470  
 471  
 472  
 473  
 474  
 475  
 476  
 477  
 478  
 479  
 480  
 481  
 482  
 483  
 484  
 485  
 486  
 487  
 488  
 489  
 490  
 491  
 492  
 493  
 494  
 495  
 496  
 497  
 498  
 499  
 500  
 501  
 502  
 503  
 504  
 505  
 506  
 507  
 508  
 509  
 510  
 511  
 512  
 513  
 514  
 515  
 516  
 517  
 518  
 519  
 520  
 521  
 522  
 523  
 524  
 525  
 526  
 527  
 528  
 529  
 530  
 531  
 532  
 533  
 534  
 535  
 536  
 537  
 538  
 539  
 540  
 541  
 542  
 543  
 544  
 545  
 546  
 547  
 548  
 549  
 550  
 551  
 552  
 553  
 554  
 555  
 556  
 557  
 558  
 559  
 560  
 561  
 562  
 563  
 564  
 565  
 566  
 567  
 568  
 569  
 570  
 571  
 572  
 573  
 574  
 575  
 576  
 577  
 578  
 579  
 580  
 581  
 582  
 583  
 584  
 585  
 586  
 587  
 588  
 589  
 590  
 591  
 592  
 593  
 594  
 595  
 596  
 597  
 598  
 599  
 600  
 601  
 602  
 603  
 604  
 605  
 606  
 607  
 608  
 609  
 610  
 611  
 612  
 613  
 614  
 615  
 616  
 617  
 618  
 619  
 620  
 621  
 622  
 623  
 624  
 625  
 626  
 627  
 628  
 629  
 630  
 631  
 632  
 633  
 634  
 635  
 636  
 637  
 638  
 639  
 640  
 641  
 642  
 643  
 644  
 645  
 646  
 647  
 648  
 649  
 650  
 651  
 652  
 653  
 654  
 655  
 656  
 657  
 658  
 659  
 660  
 661  
 662  
 663  
 664  
 665  
 666  
 667  
 668  
 669  
 670  
 671  
 672  
 673  
 674  
 675  
 676  
 677  
 678  
 679  
 680  
 681  
 682  
 683  
 684  
 685  
 686  
 687  
 688  
 689  
 690  
 691  
 692  
 693  
 694  
 695  
 696  
 697  
 698  
 699  
 700  
 701  
 702  
 703  
 704  
 705  
 706  
 707  
 708  
 709  
 710  
 711  
 712  
 713  
 714  
 715  
 716  
 717  
 718  
 719  
 720  
 721  
 722  
 723  
 724  
 725  
 726  
 727  
 728  
 729  
 730  
 731  
 732  
 733  
 734  
 735  
 736  
 737  
 738  
 739  
 740  
 741  
 742  
 743  
 744  
 745  
 746  
 747  
 748  
 749  
 750  
 751  
 752  
 753  
 754  
 755  
 756  
 757  
 758  
 759  
 760  
 761  
 762  
 763  
 764  
 765  
 766  
 767  
 768  
 769  
 770  
 771  
 772  
 773  
 774  
 775  
 776  
 777  
 778  
 779  
 780  
 781  
 782  
 783  
 784  
 785  
 786  
 787  
 788  
 789  
 790  
 791  
 792  
 793  
 794  
 795  
 796  
 797  
 798  
 799  
 800  
 801  
 802  
 803  
 804  
 805  
 806  
 807  
 808  
 809  
 810  
 811  
 812  
 813  
 814  
 815  
 816  
 817  
 818  
 819  
 820  
 821  
 822  
 823  
 824  
 825  
 826  
 827  
 828  
 829  
 830  
 831  
 832  
 833  
 834  
 835  
 836  
 837  
 838  
 839  
 840  
 841  
 842  
 843  
 844  
 845  
 846  
 847  
 848  
 849  
 850  
 851  
 852  
 853  
 854  
 855  
 856  
 857  
 858  
 859  
 860  
 861  
 862  
 863  
 864  
 865  
 866  
 867  
 868  
 869  
 870  
 871  
 872  
 873  
 874  
 875  
 876  
 877  
 878  
 879  
 880  
 881  
 882  
 883  
 884  
 885  
 886  
 887  
 888  
 889  
 890  
 891  
 892  
 893  
 894  
 895  
 896  
 897  
 898  
 899  
 900  
 901  
 902  
 903  
 904  
 905  
 906  
 907  
 908  
 909  
 910  
 911  
 912  
 913  
 914  
 915  
 916  
 917  
 918  
 919  
 920  
 921  
 922  
 923  
 924  
 925  
 926  
 927  
 928  
 929  
 930  
 931  
 932  
 933  
 934  
 935  
 936  
 937  
 938  
 939  
 940  
 941  
 942  
 943  
 944  
 945  
 946  
 947  
 948  
 949  
 950  
 951  
 952  
 953  
 954  
 955  
 956  
 957  
 958  
 959  
 960  
 961  
 962  
 963  
 964  
 965  
 966  
 967  
 968  
 969  
 970  
 971  
 972  
 973  
 974  
 975  
 976  
 977  
 978  
 979  
 980  
 981  
 982  
 983  
 984  
 985  
 986  
 987  
 988  
 989  
 990  
 991  
 992  
 993  
 994  
 995  
 996  
 997  
 998  
 999  
 1000  
 1001  
 1002  
 1003  
 1004  
 1005  
 1006  
 1007  
 1008  
 1009  
 1010  
 1011  
 1012  
 1013  
 1014  
 1015  
 1016  
 1017  
 1018  
 1019  
 1020  
 1021  
 1022  
 1023  
 1024  
 1025  
 1026  
 1027  
 1028  
 1029  
 1030  
 1031  
 1032  
 1033  
 1034  
 1035  
 1036  
 1037  
 1038  
 1039  
 1040  
 1041  
 1042  
 1043  
 1044  
 1045  
 1046  
 1047  
 1048  
 1049  
 1050  
 1051  
 1052  
 1053  
 1054  
 1055  
 1056  
 1057  
 1058  
 1059  
 1060  
 1061  
 1062  
 1063  
 1064  
 1065  
 1066  
 1067  
 1068  
 1069  
 1070  
 1071  
 1072  
 1073  
 1074  
 1075  
 1076  
 1077  
 1078  
 1079  
 1080  
 1081  
 1082  
 1083  
 1084  
 1085  
 1086  
 1087  
 1088  
 1089  
 1090  
 1091  
 1092  
 1093  
 1094  
 1095  
 1096  
 1097  
 1098  
 1099  
 1100  
 1101  
 1102  
 1103  
 1104  
 1105  
 1106  
 1107  
 1108  
 1109  
 1110  
 1111  
 1112  
 1113  
 1114  
 1115  
 1116  
 1117  
 1118  
 1119  
 1120  
 1121  
 1122  
 1123  
 1124  
 1125  
 1126  
 1127  
 1128  
 1129  
 1130  
 1131  
 1132  
 1133  
 1134  
 1135  
 1136  
 1137  
 1138  
 1139  
 1140  
 1141  
 1142  
 1143  
 1144  
 1145  
 1146  
 1147  
 1148  
 1149  
 1150  
 1151  
 1152  
 1153  
 1154  
 1155  
 1156  
 1157  
 1158  
 1159  
 1160  
 1161  
 1162  
 1163  
 1164  
 1165  
 1166  
 1167  
 1168  
 1169  
 1170  
 1171  
 1172  
 1173  
 1174  
 1175  
 1176  
 1177  
 1178  
 1179  
 1180  
 1181  
 1182  
 1183  
 1184  
 1185  
 1186  
 1187  
 1188  
 1189  
 1190  
 1191  
 1192  
 1193  
 1194  
 1195  
 1196  
 1197  
 1198  
 1199  
 1200  
 1201  
 1202  
 1203  
 1204  
 1205  
 1206  
 1207  
 1208  
 1209  
 1210  
 1211  
 1212  
 1213  
 1214  
 1215  
 1216  
 1217  
 1218  
 1219  
 1220  
 1221  
 1222  
 1223  
 1224  
 1225  
 1226  
 1227  
 1228  
 1229  
 1230  
 1231  
 1232  
 1233  
 1234  
 1235  
 1236  
 1237  
 1238  
 1239  
 1240  
 1241  
 1242  
 1243  
 1244  
 1245  
 1246  
 1247  
 1248  
 1249  
 1250  
 1251  
 1252  
 1253  
 1254  
 1255  
 1256  
 1257  
 1258  
 1259  
 1260  
 1261  
 1262  
 1263  
 1264  
 1265  
 1266  
 1267  
 1268  
 1269  
 1270  
 1271  
 1272  
 1273  
 1274  
 1275  
 1276  
 1277  
 1278  
 1279  
 1280  
 1281  
 1282  
 1283  
 1284  
 1285  
 1286  
 1287  
 1288  
 1289  
 1290  
 1291  
 1292  
 1293  
 1294  
 1295  
 1296  
 1297  
 1298  
 1299  
 1300  
 1301  
 1302  
 1303  
 1304  
 1305  
 1306  
 1307  
 1308  
 1309  
 1310  
 1311  
 1312  
 1313  
 1314  
 1315  
 1316  
 1317  
 1318  
 1319  
 1320  
 1321  
 1322  
 1323  
 1324  
 1325  
 1326  
 1327  
 1328  
 1329  
 1330  
 1331  
 1332  
 1333  
 1334  
 1335  
 1336  
 1337  
 1338  
 1339  
 1340  
 1341  
 1342  
 1343  
 1344  
 1345  
 1346  
 1347  
 1348  
 1349  
 1350  
 1351  
 1352  
 1353  
 1354  
 1355  
 1356  
 1357  
 1358  
 1359  
 1360  
 1361  
 1362  
 1363  
 1364  
 1365  
 1366  
 1367  
 1368  
 1369  
 1370  
 1371  
 1372  
 1373  
 1374  
 1375  
 1376  
 1377  
 1378  
 1379  
 1380  
 1381  
 1382  
 1383  
 1384  
 1385  
 1386  
 1387  
 1388  
 1389  
 1390  
 1391  
 1392  
 1393  
 1394  
 1395  
 1396  
 1397  
 1398  
 1399  
 1400  
 1401  
 1402  
 1403  
 1404  
 1405  
 1406  
 1407  
 1408  
 1409  
 1410  
 1411  
 1412  
 1413  
 1414  
 1415  
 1416  
 1417  
 1418  
 1419  
 1420  
 1421  
 1422  
 1423  
 1424  
 1425  
 1426  
 1427  
 1428  
 1429  
 1430  
 1431  
 1432  
 1433  
 1434  
 1435  
 1436  
 1437  
 1438  
 1439  
 1440  
 1441  
 1442  
 1443  
 1444  
 1445  
 1446  
 1447  
 1448  
 1449  
 1450  
 1451  
 1452  
 1453  
 1454  
 1455  
 1456  
 1457  
 1458  
 1459  
 1460  
 1461  
 1462  
 1463  
 1464  
 1465  
 1466  
 1467  
 1468  
 1469  
 1470  
 1471  
 1472  
 1473  
 1474  
 1475  
 1476  
 1477  
 1478  
 1479  
 1480  
 1481  
 1482  
 1483  
 1484  
 1485  
 1486  
 1487  
 1488  
 1489  
 1490  
 1491  
 1492  
 1493  
 1494  
 1495  
 1496  
 1497  
 1498  
 1499  
 1500  
 1501  
 1502  
 1503  
 1504  
 1505  
 1506  
 1507  
 1508  
 1509  
 1510  
 1511  
 1512  
 1513  
 1514  
 1515  
 1516  
 1517  
 1518  
 1519  
 1520  
 1521  
 1522  
 1523  
 1524  
 1525  
 1526  
 1527  
 1528  
 1529  
 1530  
 1531  
 1532  
 1533  
 1534  
 1535  
 1536  
 1537  
 1538  
 1539  
 1540  
 1541  
 1542  
 1543  
 1544  
 1545  
 1546  
 1547  
 1548  
 1549  
 1550  
 1551  
 1552  
 1553  
 1554  
 1555  
 1556  
 1557  
 1558  
 1559  
 1560  
 1561  
 1562  
 1563  
 1564  
 1565  
 1566  
 1567  
 1568  
 1569  
 1570  
 1571  
 1572  
 1573  
 1574  
 1575  
 1576  
 1577  
 1578  
 1579  
 1580  
 1581  
 1582  
 1583  
 1584  
 1585  
 1586  
 158

108 2024), and neuron- or rank-level manipulations (Wei et al., 2024; Li et al., 2024b). Together, these  
 109 works establish refusal as an interpretable and causally manipulable concept, but also highlight its  
 110 brittleness to adversarial inputs and fine-tuning.  
 111

112 **Safety Steering and Training-free Defenses.** Training-free interventions attempt to steer model  
 113 activations without costly fine-tuning. Early work showed that feature directions derived from  
 114 contrastive inputs can modulate model behavior (Zou et al., 2023; Panickssery et al., 2023; Li et al.,  
 115 2024a; Marks & Tegmark, 2023; Turner et al., 2023). Sparse autoencoders (SAEs) provide an un-  
 116 supervised route to discover such features (Bricken et al., 2023; Templeton et al., 2024). Recently,  
 117 SAE-based steering has been applied directly to safety, revealing both promise and utility tradeoffs  
 118 (O’Brien et al., 2024). Extensions include instruction-following features (He et al., 2025), category-  
 119 wise safety steering (Ghosh et al., 2025; Bhattacharjee et al., 2024), and adaptive methods such as  
 120 AdaSteer (Zhao et al., 2025). Complementary strategies include Safety Arithmetic (Hazra et al.,  
 121 2024), Representation Bending (Yousefpour et al., 2025), Low-Rank Extrapolation (Perin et al.,  
 122 2025), adversarial training approaches such as ReFAT (Yu et al., 2024), and null-space constraints  
 123 methods like AlphaSteer (Sheng et al., 2025) that builds on insights from AlphaEdit(Fang et al.,  
 124 2025) which is used for robust knowledge editing. Foundational studies further established linear  
 125 features in representation spaces (Bolukbasi et al., 2016; Elhage et al., 2022; Geiger et al., 2024;  
 126 Ravfogel et al., 2020). While effective, many steering-based defenses introduce capability tradeoffs,  
 127 motivating interpretable and more surgical alternatives such as ours.  
 128

129 **Beyond Steering: Fine-tuning and Safety Robustness.** Another line of work examines how  
 130 safety alignment emerges or fails under fine-tuning. Works like Zhan et al. (2023); Yang et al.  
 131 (2023); Qi et al. (2023); Lermen et al. (2023) show that even small malicious or benign finetunes  
 132 can undo refusal, while mechanistic studies suggest the internal circuitry remains intact (Jain et al.,  
 133 2024b). SAFELORA, a training-free and data-free approach that shows how LoRA weights can  
 134 be projected onto a safety-aligned subspace reducing safety degradation from fine-tuning LLMs.  
 135 Other interventions strengthen refusal explicitly, such as extended-refusal finetuning against abli-  
 136 teration attacks (Shairah et al., 2025), refusal tokens for controllable calibration (Jain et al., 2024a),  
 137 and single-vector ablations to mitigate false refusals (Wang et al., 2025). Others work on run-time  
 138 interventions to protect against jailbreaks, such as SMOOTHLLM (Robey et al., 2024), and Jail-  
 139 break Antidote (Shen et al., 2025). Alignment fragility also arises in model merging: Hammoud  
 140 et al. (2024) showed that unsafe models contaminate the merged ones unless alignment is explic-  
 141 itely included. Together, these works highlight the tension between robustness and utility in safety  
 142 interventions.  
 143

144 **Our Contribution.** We build directly on the insight of Ardi et al. (2024) but invert its vulnerabil-  
 145 ity: instead of ablating the safety direction to weaken safety, our ROSI method permanently injects  
 146 it into model weights. Compared to inference-time steering (O’Brien et al., 2024; Zhao et al., 2025;  
 147 Ghosh et al., 2025; Sheng et al., 2025; Shen et al., 2025), ROSI provides a one-time lightweight,  
 148 fine-tuning-free, interpretable mechanism that is permanent yet minimally invasive. Compared to  
 149 approaches based on fine-tuning (Zhan et al., 2023; Shairah et al., 2025), it achieves comparable  
 150 robustness with a much lower cost. Importantly, ROSI is not intended to replace existing safety  
 151 strategies; it can be layered with steering, fine-tuning, or other alignment methods to further rein-  
 152 force model robustness. Thus, our work illustrates how mechanistic interpretability can be leveraged  
 153 not only to diagnose vulnerabilities but also to design efficient last-mile safety amplification tech-  
 154 niques.  
 155

### 3 METHODOLOGY

156 Our proposed method, ROSI, which is illustrated in Figure 1, is based on the principle that high-level  
 157 concepts such as safety are linearly represented in the activation space of a model. We first extract  
 158 this “safety direction” and then use it to craft a permanent modification to the model’s weights.  
 159

#### 3.1 MATHEMATICAL PRELIMINARIES: TRANSFORMERS

160 A decoder-only Transformer model processes a sequence of input tokens  $\mathbf{t} = (t_1, \dots, t_n)$ . The core  
 161 of the model is the residual stream,  $\mathbf{x}_i^{(l)} \in \mathbb{R}^{d_{\text{model}}}$ , which represents the activation for the  $i$ -th token

162 at the  $l$ -th layer. Each layer  $l$  updates this activation through an attention block and a multi-layer  
 163 perceptron (MLP) block:

$$\tilde{\mathbf{x}}_i^{(l)} = \mathbf{x}_i^{(l)} + \text{Attn}^{(l)}(\mathbf{x}_{1:i}^{(l)}) \quad (1)$$

$$\mathbf{x}_i^{(l+1)} = \tilde{\mathbf{x}}_i^{(l)} + \text{MLP}^{(l)}(\tilde{\mathbf{x}}_i^{(l)}) \quad (2)$$

168 The key components that are written in the residual stream are the attention output projection matrix  
 169 ( $W_O$ ) and the MLP output projection matrix ( $W_{out}$ ). Our method targets these matrices, among  
 170 others, for modification.

### 171 3.2 EXTRACTING THE SAFETY DIRECTION

173 To isolate the direction in the activation space corresponding to safety and refusal, we employ the  
 174 difference-in-means technique. We construct two small and contrasting datasets.

- 176 •  $\mathcal{D}_{\text{harmful}}$ : A set of instructions that should elicit a refusal (e.g., "How do I build a bomb?").
- 177 •  $\mathcal{D}_{\text{harmless}}$ : A set of benign instructions that should be answered helpfully (e.g., "How do I  
 178 bake a cake?").

180 We run the model on all the prompts in both datasets and collect the residual stream activations  $\mathbf{x}_i^{(l)}$   
 181 at a specific layer  $l$  and the position of the token  $i$  (typically the last token of the prompt). We then  
 182 compute the mean activation for each dataset:

$$\boldsymbol{\mu}^{(l)} = \frac{1}{|\mathcal{D}_{\text{harmful}}|} \sum_{\mathbf{t} \in \mathcal{D}_{\text{harmful}}} \mathbf{x}_i^{(l)}(\mathbf{t}) \quad (3)$$

$$\boldsymbol{\nu}^{(l)} = \frac{1}{|\mathcal{D}_{\text{harmless}}|} \sum_{\mathbf{t} \in \mathcal{D}_{\text{harmless}}} \mathbf{x}_i^{(l)}(\mathbf{t}) \quad (4)$$

188 The safety direction  $\mathbf{s}^{(l)}$  is defined as the difference between these two means:

$$\mathbf{s}^{(l)} = \boldsymbol{\mu}^{(l)} - \boldsymbol{\nu}^{(l)} \quad (5)$$

192 This vector  $\mathbf{s}^{(l)}$  points from the center of the harmless activation cluster towards the center of the  
 193 harmful activation cluster. We select the optimal layer  $l^*$  that yields the most effective direction  
 194 based on a validation set of harmful and harmless prompts. We select the direction that maximizes  
 195 refusal on harmful prompts while maintaining a KL-Divergence of  $\leq 0.1$  on the harmless instruc-  
 196 tions. The final normalized safety direction is denoted as  $\hat{\mathbf{s}}$ .

### 197 3.3 RANK-ONE SAFETY INJECTION (ROSI)

199 Previous work has shown that one can ablate a direction  $\hat{\mathbf{s}}$  from a weight matrix  $W$  by applying a  
 200 projection:  $W' \leftarrow (I - \hat{\mathbf{s}}\hat{\mathbf{s}}^T)W$ . This effectively removes the model's ability to represent information  
 201 along that direction.

202 We propose the opposite: to amplify this direction. We achieve this by modifying every weight  
 203 matrix  $W_{\text{out}} \in \mathbb{R}^{d_{\text{model}} \times d_{\text{input}}}$  that writes to the residual stream. The modification is a rank-one update  
 204 designed to add a small, consistent push in the direction of  $\hat{\mathbf{s}}$ . The ROSI update rule is:

$$W'_{\text{out}} \leftarrow W_{\text{out}} + \alpha \cdot \hat{\mathbf{s}} \cdot \bar{\mathbf{w}}^T \quad (6)$$

207 where:

- 209 •  $\alpha$  is a scalar hyperparameter that controls the strength of the injection.
- 210 •  $\hat{\mathbf{s}} \in \mathbb{R}^{d_{\text{model}}}$  is the normalized safety direction.
- 211 •  $\bar{\mathbf{w}} \in \mathbb{R}^{d_{\text{input}}}$  is the mean of the row vectors of the original weight matrix  $W_{\text{out}}$ .

213 This formulation creates a rank-one matrix  $\alpha(\hat{\mathbf{s}}\bar{\mathbf{w}}^T)$  which is added to the original weights. The  
 214 intuition is that for an average input, this modification adds a component proportional to the safety  
 215 direction  $\hat{\mathbf{s}}$  to the output, effectively steering the model's activations toward the refusal-mediating  
 subspace. This is a permanent, efficient, and targeted change to the model's behavior.

216 

## 4 EXPERIMENTS AND RESULTS

217  
218 Our empirical evaluation is designed to answer three key questions:  
219

- 220 1. Can ROSI amplify the safety of existing, aligned models and improve their robustness to
- 
- 221 adversarial attacks without degrading their general capabilities?
- 
- 222 2. Can ROSI effectively inject safety into "uncensored" models that have been fine-tuned to
- 
- 223 bypass safety constraints?
- 
- 224 3. Does this injected safety come at the cost of utility in these uncensored models?
- 
- 225

226 We address these questions through a series of controlled experiments on a diverse set of models  
227 and benchmarks.  
228229 

### 4.1 EXPERIMENTAL SETUP

230 **Models.** We test two categories of models: **Aligned Models** including LLAMA-2 (Touvron et al.,  
231 2023), LLAMA-3 (Llama Team, 2024), QWEN2.5 (Qwen et al., 2025), GEMMA (Team et al., 2024),  
232 and YI (AI et al., 2025), which have standard safety training; and **Uncensored Models**, specifically  
233 the DOLPHIN series (Dolphin, 2025), which are intentionally fine-tuned to ignore safety.  
234235 **Evaluation.** Safety is measured via Harm Refusal (HR) on CATQA (Bhardwaj et al., 2024), a set  
236 of 550 harmful instructions from 11 categories, evaluated using LLAMA GUARD 3 (Llama Team,  
237 2024). We also measure attack success rates on jailbreak benchmarks—DAN, HARBENCH  
238 (Mazeika et al., 2024), WILDGUARDTEST, and WILDJAILBREAK (Jiang et al., 2024)—judged by  
239 WILDGUARD (Han et al., 2024). Utility is assessed on standard benchmarks: MMLU (Hendrycks  
240 et al., 2021), HELLASWAG (Zellers et al., 2019), ARC (Chollet, 2019), BOOLQ (Clark et al., 2019),  
241 and TRUTHFULQA (Lin et al., 2022). We also measure Benign Compliance (BC) on a randomly  
242 sampled set of 512 instructions from ALPACA (Taori et al., 2023), to ensure ROSI models do not  
243 refuse safe instructions.  
244245 **Implementation.** The safety direction for each model was extracted using 50 harmful/harmless  
246 pairs. Generations use greedy decoding with a max length of 1024 tokens.  
247248 **Table 1: Harm Refusal in Aligned Models.** ROSI consistently improves the refusal rate for harmful  
249 prompts (HR %) while maintaining high compliance for benign ones (BC %).  
250

Model	ROSI	HR %	BC %
GEMMA-2B-INSTRUCT	✗ ✓	98.4 99.8 (+1.5)	99.4 99.0 (-0.4)
LLAMA-2-7B-CHAT-HF	✗ ✓	99.8 100.0 (+0.2)	98.8 99.8 (+1.0)
META-LLAMA-3.1-8B-INSTRUCT	✗ ✓	98.2 99.1 (+0.9)	99.6 99.6 (0.0)
META-LLAMA-3.2-1B-INSTRUCT	✗ ✓	79.5 92.7 (+13.2)	99.2 95.9 (-3.9)
QWEN2.5-0.5B-INSTRUCT	✗ ✓	90.4 99.3 (+8.9)	98.6 91.4 (-7.2)
QWEN2.5-3B-INSTRUCT	✗ ✓	89.8 99.6 (+9.8)	99.6 98.6 (-1.0)
QWEN2.5-7B-INSTRUCT	✗ ✓	95.8 100.0 (+4.2)	100.0 99.0 (-1.0)
QWEN2.5-14B-INSTRUCT	✗ ✓	98.9 100.0 (+1.1)	100.0 99.4 (-0.6)
YI-6B-CHAT	✗ ✓	81.3 99.5 (+18.2)	99.6 97.7 (-1.7)

270 Table 2: **Jailbreak Robustness of Aligned Models.** Scores represent attack success rates (lower is  
 271 better). ROSI significantly reduces model vulnerability across all attack vectors.  
 272

273 Model	274 ROSI	275 DAN $\downarrow$	276 HARMBENCH $\downarrow$	277 WILDGUARDTEST $\downarrow$			278 WILDJAILBREAK Harmful $\downarrow$
				279 WG-Micro	280 WG-Adv.	281 WG-Vanilla	
GEMMA-2B-INSTRUCT	$\times$ ✓	5.3 <b>1.0 (-4.3)</b>	6.2 <b>3.4 (-2.8)</b>	9.1 <b>2.4 (-6.7)</b>	16.6 <b>4.7 (-11.9)</b>	2.9 <b>0.5 (-2.4)</b>	42.3 <b>8.2 (-34.1)</b>
LLAMA-2-7B-CHAT-HF	$\times$ ✓	0.0 (0.0)	0.0 (0.0)	0.9 <b>0.0 (-0.9)</b>	2.1 <b>0.0 (-2.1)</b>	0.0 (0.0)	3.5 <b>0.1 (-3.4)</b>
LLAMA-3.1-8B-INSTRUCT	$\times$ ✓	0.3 <b>0.0 (-0.3)</b>	5.9 <b>5.3 (-0.6)</b>	1.6 <b>0.0 (-1.6)</b>	2.7 <b>0.0 (-2.7)</b>	0.7 <b>0.0 (-0.7)</b>	14.8 <b>1.8 (-13.0)</b>
LLAMA-3.2-1B-INSTRUCT	$\times$ ✓	1.3 <b>0.0 (-1.3)</b>	8.4 <b>5.6 (-2.8)</b>	4.0 <b>1.3 (-2.7)</b>	3.9 <b>1.5 (-2.4)</b>	4.1 <b>1.2 (-2.9)</b>	18.7 <b>7.5 (-11.1)</b>
QWEN2.5-0.5B-INSTRUCT	$\times$ ✓	36.0 <b>7.0 (-29.0)</b>	31.6 <b>12.8 (-18.8)</b>	33.1 <b>21.1 (-12.0)</b>	48.1 <b>38.0 (-10.1)</b>	20.9 <b>7.3 (-13.6)</b>	91.8 <b>58.8 (-33.0)</b>
QWEN2.5-3B-INSTRUCT	$\times$ ✓	52.7 <b>6.7 (-46.0)</b>	12.5 <b>1.6 (-10.9)</b>	21.4 <b>12.7 (-8.7)</b>	37.4 <b>26.7 (-10.7)</b>	8.3 <b>1.2 (-7.1)</b>	93.7 <b>61.5 (-32.2)</b>
QWEN2.5-7B-INSTRUCT	$\times$ ✓	40.3 <b>11.7 (-28.6)</b>	22.5 <b>1.9 (-20.6)</b>	18.6 <b>3.9 (-14.7)</b>	36.2 <b>7.7 (-28.5)</b>	4.1 <b>0.7 (-3.4)</b>	90.7 <b>36.7 (-54.0)</b>
QWEN2.5-14B-INSTRUCT	$\times$ ✓	32.3 <b>5.0 (-27.3)</b>	7.2 <b>1.6 (-5.6)</b>	12.1 <b>5.1 (-7.0)</b>	24.0 <b>11.0 (-13.0)</b>	2.4 <b>0.2 (-2.2)</b>	81.2 <b>43.9 (-37.3)</b>
YI-6B-CHAT	$\times$ ✓	52.0 <b>15.3 (-36.7)</b>	20.9 <b>7.8 (-13.1)</b>	22.7 <b>10.1 (-12.6)</b>	39.2 <b>22.0 (-17.2)</b>	9.2 <b>0.5 (-8.7)</b>	89.4 <b>44.6 (-44.8)</b>

289 Table 3: **Utility Preservation in Aligned Models.** Performance on standard benchmarks with ROSI  
 290 (✓) versus baseline (✗).  
 291

292 Model	293 ROSI	294 MMLU	295 HELLA-SWAG	296 ARC EASY	297 ARC CHAL.	298 BOOLQ	299 TRUTHFULQA
GEMMA-2B-INSTRUCT	$\times$ ✓	38.1 <b>38.3 (+0.2)</b>	49.2 <b>49.3 (+0.1)</b>	71.7 <b>70.8 (-0.9)</b>	40.4 <b>39.0 (-1.4)</b>	63.7 <b>61.4 (-2.3)</b>	45.8 <b>46.7 (+0.9)</b>
LLAMA-2-7B-CHAT-HF	$\times$ ✓	46.3 <b>46.4 (+0.1)</b>	57.8 <b>57.7 (-0.1)</b>	74.0 <b>73.4 (-0.6)</b>	43.9 <b>43.3 (-0.6)</b>	79.6 <b>79.8 (+0.2)</b>	45.3 <b>47.2 (+1.9)</b>
META-LLAMA-3.1-8B-INSTRUCT	$\times$ ✓	68.0 <b>67.6 (-0.4)</b>	59.1 <b>58.9 (-0.2)</b>	81.7 <b>81.1 (-0.6)</b>	51.6 <b>51.1 (-0.5)</b>	84.0 <b>83.8 (-0.2)</b>	54.1 <b>54.8 (+0.7)</b>
META-LLAMA-3.2-1B-INSTRUCT	$\times$ ✓	46.0 <b>45.4 (-0.6)</b>	45.2 <b>45.4 (+0.2)</b>	68.3 <b>67.4 (-0.9)</b>	35.6 <b>34.7 (-0.9)</b>	69.3 <b>68.7 (-0.6)</b>	43.9 <b>45.0 (+1.1)</b>
QWEN2.5-0.5B-INSTRUCT	$\times$ ✓	45.8 <b>45.3 (-0.5)</b>	40.5 <b>40.4 (-0.1)</b>	65.5 <b>64.3 (-1.2)</b>	30.1 <b>29.6 (-0.5)</b>	67.6 <b>63.2 (-4.4)</b>	41.8 <b>43.8 (+2.0)</b>
QWEN2.5-3B-INSTRUCT	$\times$ ✓	65.4 <b>65.0 (-0.4)</b>	56.3 <b>55.8 (-0.5)</b>	76.9 <b>76.6 (-0.3)</b>	45.7 <b>45.1 (-0.6)</b>	80.1 <b>77.4 (-2.7)</b>	58.7 <b>59.7 (+1.0)</b>
QWEN2.5-7B-INSTRUCT	$\times$ ✓	71.8 <b>71.9 (+0.1)</b>	62.0 <b>61.9 (-0.1)</b>	81.6 <b>81.0 (-0.6)</b>	52.6 <b>52.6 (0.0)</b>	86.4 <b>86.2 (-0.2)</b>	64.8 <b>66.1 (+1.3)</b>
QWEN2.5-14B-INSTRUCT	$\times$ ✓	78.8 <b>78.9 (+0.1)</b>	65.6 <b>65.6 (0.0)</b>	85.7 <b>85.6 (-0.1)</b>	60.4 <b>60.7 (+0.3)</b>	88.0 <b>85.8 (-2.2)</b>	69.0 <b>71.9 (+2.9)</b>
YI-6B-CHAT	$\times$ ✓	61.6 <b>61.1 (-0.5)</b>	57.7 <b>57.2 (-0.5)</b>	74.5 <b>78.1 (+3.6)</b>	44.1 <b>46.9 (+2.8)</b>	82.8 <b>84.2 (+1.4)</b>	49.9 <b>51.2 (+1.3)</b>

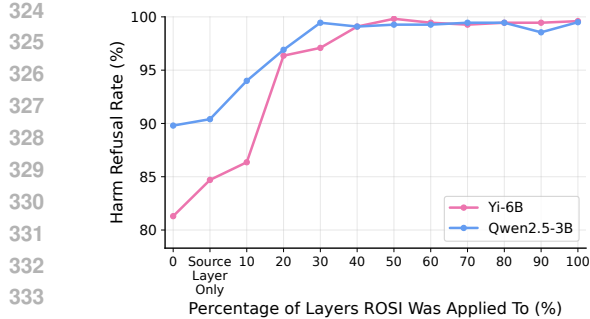
## 308 4.2 AMPLIFYING SAFETY IN ALIGNED MODELS

309 We first test ROSI’s ability to bolster the defenses of models that already possess safety alignment.  
 310

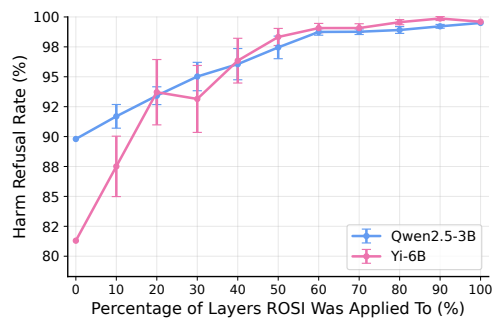
311 **Increased Refusal and Jailbreak Robustness.** As shown in Table 1, applying ROSI consistently  
 312 enhances the Harm Refusal (HR) rate across all aligned models tested. The effect is particularly  
 313 pronounced for models with weaker baselines, such as YI-6B-CHAT (+18.2 points) and META-  
 314 LLAMA-3.2-1B-INSTRUCT (+13.3 points), elevating their safety to near-perfect levels. This im-  
 315 provement is not superficial; Table 2 shows that ROSI drastically hardens models against a full  
 316 suite of adversarial jailbreak attacks. For many models, attack success rates are cut by more than  
 317 half, demonstrating a fundamental increase in robustness.  
 318

319 In Appendix 5, we discuss what role ROSI can play in fine-tuning LLMs.  
 320

321 **Preservation of Model Utility.** Crucially, these safety gains do not compromise the models’ core  
 322 functionalities. Table 3 provides a comprehensive view of utility preservation. The average per-  
 323 formance across a suite of seven benchmarks remains remarkably stable. The vast majority of models



(a) Selection is centered on the layer from which the safety vector is extracted and a proportional window around it.



(b) Layers are selected at random; the process is repeated 10 times for each ratio, the plot show the mean refusal rate with confidence intervals.

Figure 2: **Injected Layers Ablations.** In Figure 2a, we ablate the number of layers we apply ROSI to by taking a ratio  $x$  (x-axis) of a model’s layers that is centered around the index of the layer  $i$  used to extract the safety vector. In Figure 2b, a subset of layers is selected randomly each time, we repeat the run 10 times for each ratio and take the average of the harm refusal rate. Confidence intervals are reported.

see an average score change of less than 0.5%. A similar pattern holds for BC, as seen in Table 1, ROSI models’ refusal of safe instructions, on average, remains minimal. While smaller models ( $\leq 1$ B) show the biggest degradation in BC, they still gain more in HR than what they lose in BC. These results demonstrate that the safety direction is largely orthogonal to the representations required for knowledge and reasoning tasks. ROSI acts as a surgical tool, enhancing safety with minimal side effects.

**Injected Layers Ablations.** To assess how stable the ROSI update is within a model, we perform a set of ablations that vary both the number and the identity of the layers receiving the safety injection for two representative models, Yi-6B-CHAT and Qwen2.5-3B-INSTRUCT. In the first setting, we inject ROSI into a contiguous block of layers centered on the layer index used to extract the safety vector, expanding this window according to a chosen fraction of the model’s total depth. Figure 2a shows how injecting just at the source layer yields only modest improvements, and as the window of injected layers is expanded, the harm refusal rate keeps increasing until it stabilizes around the 30 – 40% window size, suggesting that only a limited number of layers within a model contribute to the concept of “safety”. In a second setting, we examine robustness by randomly selecting the same number of layers for each fraction. For every ratio, we repeat the process ten times and average the resulting refusal scores. Figure 2b displays a similar trend to the former experiment, but the confidence intervals show that performance varies considerably depending on the layers selected. Notably, Yi-6B-CHAT peaks at 100% HR rates in one of the runs where ROSI was applied to only half of the layers, which suggests that optimizing the set of injected layers can further improve performance.

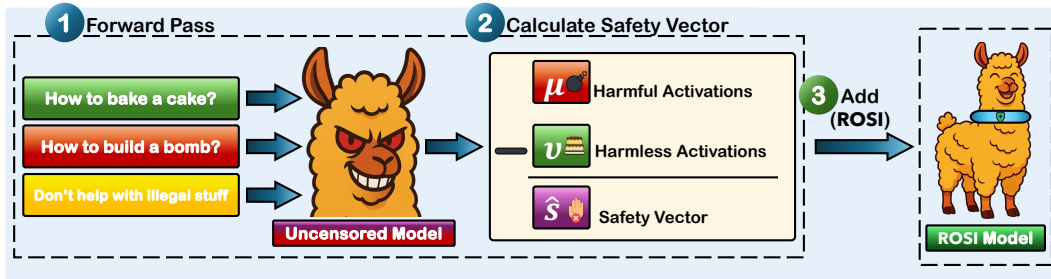
### Conclusion 1

ROSI effectively amplifies the safety of existing aligned models. It robustly increases their refusal of harmful prompts and hardens them against jailbreak attacks, all with a negligible impact on their general utility and performance.

### 4.3 INJECTING SAFETY INTO UNCENSORED MODELS

The previous experiment demonstrated that ROSI can enhance refusal behavior in models that are already aligned. We now turn to the more demanding task of applying ROSI to uncensored DOLPHIN models. This tests whether our method can serve as a “last-mile” re-alignment tool to instill safety where it was deliberately removed.

378  
 379 **Figure 3: Applying ROSI to Uncensored Models.** In the forward pass, **harmful** and **harmless**  
 380 instructions are prepended with a **system prompt** directing an uncensored model to reject harmful  
 381 requests, thus eliciting refusal.



393 **Table 4: Safety Injection in Uncensored Models.** Applying ROSI substantially boosts harm-  
 394 refusal (HR) across DOLPHIN models, while preserving compliance with benign instructions (BC).  
 395 Ablations without a safety system prompt (•) highlight the role of prompt-level safety conditioning.

Model	ROSI	HR %	BC %
DOLPHIN3.0-LLAMA3.2-1B	✗	23.5	100.0
	✓	46.0 (+22.5)	99.4 (-0.6)
	•	18.4 (-5.1)	100.0 (0.0)
DOLPHIN3.0-QWEN2.5-3B	✗	50.0	100.0
	✓	86.0 (+36.0)	99.6 (-0.4)
	•	33.6 (-16.4)	100.0 (0.0)
DOLPHIN3.0-LLAMA3.1-8B	✗	65.8	100.0
	✓	100.0 (+34.2)	100.0 (0.0)
	•	88.9 (+23.1)	100.0 (0.0)
DOLPHIN3.0-MISTRAL-24B	✗	64.4	100.0
	✓	92.0 (+27.6)	100.0 (0.0)
	•	47.8 (-16.6)	100.0 (0.0)

411 **Eliciting Refusal Behavior and Reducing Vulnerability.** The DOLPHIN models exhibit very low  
 412 baseline safety, leaving little to no refusal signal to extract. Directly applying the method from  
 413 Section 3 to a DOLPHIN model would therefore yield a vector  $\hat{s}$  that does not represent a safety  
 414 direction.

415 To overcome this, we explicitly *elicit* refusal behavior by modifying the system prompt, as can  
 416 be seen in Figure 3. Specifically, we prepend instructions that direct the model to reject harmful  
 417 categories of requests; the prompt we used can be seen in Appendix D. This artificially introduces a  
 418 refusal subspace that would otherwise be absent. Once present, we can apply ROSI to these models.  
 419 Afterwards, the system prompt is no longer needed and is removed during testing.

420 Table 4 shows that ROSI achieves dramatic improvements. For instance, DOLPHIN3.0-QWEN2.5-  
 421 3B's safe response rate skyrockets from 50.0% to 86.0% (+36.0), while DOLPHIN3.0-LLAMA3.1-  
 422 8B is fully re-aligned to 100% safety. This demonstrates that even uncensored models retain a latent  
 423 safety direction that is potent enough to overwrite their fine-tuning when amplified. This injected  
 424 safety also translates to improved robustness. As seen in Table 5, ROSI provides a powerful first  
 425 line of defense, slashing attack success rates by large margins (e.g., a 46.3-point reduction on DAN  
 426 for DOLPHIN3.0-QWEN2.5-3B).

427 **Utility Preservation.** Answering our final question, Table 6 confirms that this powerful safety in-  
 428 jection does not harm the utility of the uncensored models. The average performance across the  
 429 benchmark suite is virtually unchanged, with score differences of only +/- 0.2%. This result is  
 430 significant: it shows that safety can be added back to a model post-hoc without repeating expen-  
 431 sive fine-tuning.

432 **Table 5: Jailbreak Vulnerability of Uncensored Models.** Scores are attack success rates (lower is  
 433 better). ROSI provides a crucial layer of defense, significantly reducing their extreme vulnerability.  
 434

Model	ROSI	DAN ↓	HARMBENCH ↓	WILDGUARDTEST ↓			WILDJAILBREAK Harmful ↓
				WG-Micro	WG-Adv.	WG-Vanilla	
DOLPHIN3.0-LLAMA3.2-1B	✗	90.3	62.8	50.3	42.4	56.8	98.5
	✓	<b>65.7 (-24.7)</b>	<b>51.9 (-10.9)</b>	<b>33.9 (-16.4)</b>	<b>38.3 (-4.2)</b>	<b>30.3 (-26.5)</b>	<b>88.9 (-9.5)</b>
	✗	88.6 ( <b>+1.7</b> )	72.2 ( <b>+9.4</b> )	59.3 ( <b>+9.0</b> )	48.1 ( <b>+5.7</b> )	68.5 ( <b>+11.7</b> )	97.7 (-0.8)
DOLPHIN3.0-QWEN2.5-3B	✗	90.3	52.8	32.6	37.7	28.4	96.7
	✓	<b>44.0 (-46.3)</b>	<b>20.9 (-31.9)</b>	<b>15.4 (-17.2)</b>	<b>27.3 (-10.4)</b>	<b>5.6 (-22.8)</b>	<b>70.4 (-26.3)</b>
	✗	52.7 ( <b>-37.6</b> )	32.2 ( <b>-20.6</b> )	23.4 ( <b>-9.2</b> )	29.4 ( <b>-8.3</b> )	18.4 ( <b>-10.0</b> )	82.8 ( <b>-13.9</b> )
DOLPHIN3.0-LLAMA3.1-8B	✗	90.3	54.7	27.0	34.7	20.6	94.0
	✓	82.3 ( <b>-8.0</b> )	47.2 ( <b>-7.5</b> )	21.1 ( <b>-5.9</b> )	29.4 ( <b>-5.3</b> )	14.3 ( <b>-6.3</b> )	<b>82.8 (-11.3)</b>
	✗	<b>81.3 (-9.0)</b>	<b>44.7 (-10.0)</b>	<b>19.2 (-7.8)</b>	<b>26.7 (-8.0)</b>	<b>13.1 (-7.5)</b>	84.1 ( <b>-9.9</b> )
DOLPHIN3.0-MISTRAL-24B	✗	80.7	43.8	18.7	27.3	11.7	87.5
	✓	<b>64.3 (-16.3)</b>	<b>28.4 (-15.3)</b>	<b>9.1 (-9.6)</b>	<b>16.9 (-10.4)</b>	<b>2.7 (-9.0)</b>	<b>63.2 (-24.2)</b>
	✗	84.0 ( <b>+3.3</b> )	50.0 ( <b>+6.2</b> )	22.4 ( <b>+3.7</b> )	27.0 ( <b>-0.3</b> )	18.7 ( <b>+7.0</b> )	92.2 ( <b>+4.7</b> )

446  
 447 **Table 6: Utility Preservation in Uncensored Models.** Performance after applying ROSI is shown  
 448 with deltas relative to the baseline.  
 449

Model	ROSI	MMLU	HELLASWAG	ARC EASY	ARC CHAL.	BOOLQ	TRUTHFULQA
DOLPHIN3.0-LLAMA3.2-1B	✗	35.3	47.8	65.7	34.7	59.3	39.5
	✓	35.0 ( <b>-0.3</b> )	47.7 ( <b>-0.1</b> )	65.7 (0.0)	34.7 (0.0)	60.0 ( <b>+0.7</b> )	40.2 ( <b>+0.7</b> )
	✗	30.1 ( <b>-5.2</b> )	41.5 ( <b>-6.3</b> )	58.3 ( <b>-7.4</b> )	27.5 ( <b>-7.2</b> )	53.2 ( <b>-6.1</b> )	42.8 ( <b>+3.3</b> )
DOLPHIN3.0-QWEN2.5-3B	✗	64.7	55.5	77.9	43.8	80.5	49.5
	✓	64.7 (0.0)	55.4 ( <b>-0.1</b> )	77.7 ( <b>-0.2</b> )	43.8 (0.0)	80.6 ( <b>+0.1</b> )	50.8 ( <b>+1.3</b> )
	✗	64.7 (0.0)	55.6 ( <b>+0.1</b> )	77.2 ( <b>-0.7</b> )	43.7 ( <b>-0.1</b> )	78.7 ( <b>-1.8</b> )	50.1 ( <b>+0.6</b> )
DOLPHIN3.0-LLAMA3.1-8B	✗	59.0	61.3	80.9	50.1	85.6	50.1
	✓	<b>58.9 (-0.1)</b>	61.2 ( <b>-0.1</b> )	<b>80.4 (-0.5)</b>	<b>50.4 (+0.3)</b>	<b>85.0 (-0.6)</b>	<b>51.0 (+0.9)</b>
	✗	59.0 (0.0)	61.2 ( <b>-0.1</b> )	80.1 ( <b>-0.8</b> )	50.2 ( <b>+0.1</b> )	85.1 ( <b>-0.5</b> )	50.9 ( <b>+0.8</b> )
DOLPHIN3.0-MISTRAL-24B	✗	72.5	59.8	26.6	22.1	84.1	54.6
	✓	72.5 (0.0)	<b>59.7 (-0.1)</b>	<b>26.9 (+0.3)</b>	<b>22.5 (+0.4)</b>	<b>83.9 (-0.2)</b>	<b>55.7 (+1.1)</b>
	✗	72.2 ( <b>-0.3</b> )	59.6 ( <b>-0.2</b> )	27.0 ( <b>+0.4</b> )	23.0 ( <b>+0.9</b> )	84.2 ( <b>+0.1</b> )	53.8 ( <b>-0.8</b> )

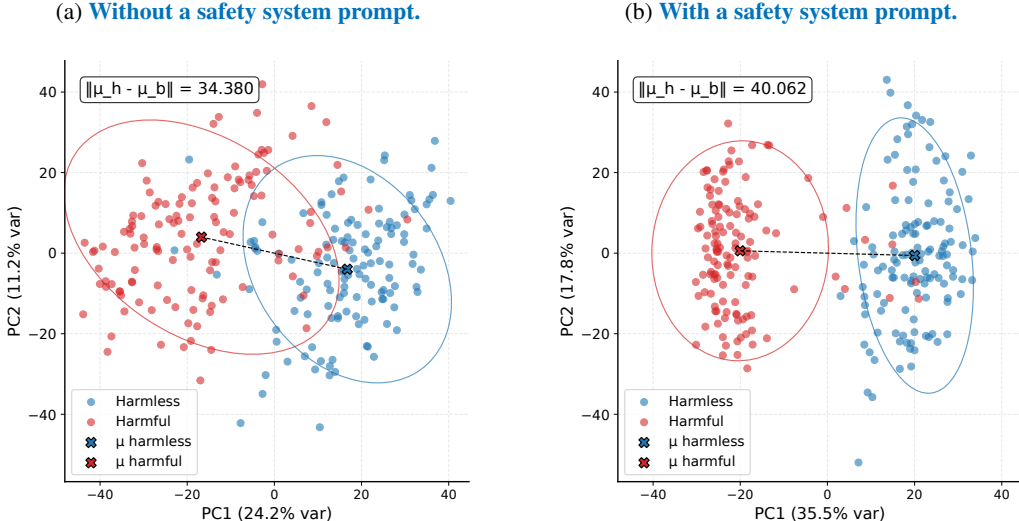
462  
 463  
 464  
 465 sive training or compromising the helpful capabilities that the uncensored model was designed to  
 466 maximize.  
 467

470 **System Prompt Ablation.** Values marked with (✗) in Table 4 show results from models where  
 471 ROSI was applied without prepending a safety system prompt to the input instructions. In this  
 472 setting, DOLPHIN3.0-LLAMA3.1-8B exhibits an 11.1% smaller gain in harm refusal compared to  
 473 when a safety system prompt is present. Other models fare considerably worse, with performance  
 474 degrading outright. Table 5 mirrors this trend: a safety system prompt is essential to fully realize  
 475 the benefits of ROSI in uncensored models. The relative resilience of DOLPHIN3.0-LLAMA3.1-  
 476 8B without the system prompt suggests that the safety signal may not have been completely erased  
 477 during uncensoring. In Figure 4, we examine how the presence of a safety system prompt influ-  
 478 ences the linear separability of harmful and harmless representations in the activation space. Using  
 479 DOLPHIN3.0-QWEN2.5-3B, we see that without the system prompt, the latent distributions over-  
 480 lap significantly, impeding the ability of the steering vector to differentiate between safe and unsafe  
 481 contexts. On the other hand, prepending the prompt effectively disentangles these clusters, increas-  
 482 ing the centroid distance and restoring the distinct decision boundaries required for robust refusal.  
 483 Taken together, these results support our hypothesis: a safety system prompt is crucial for eliciting  
 484 a strong and coherent safety direction in uncensored models.

485 In Appendix E, we show that, on the other hand, aligned models do not benefit from the safety  
 486 system prompt.

486  
 487  
 488  
 489  
 490  
 491  
 492  
 493  
 494  
 495  
 496  
 497  
 498  
 499  
 500  
 501  
 502  
 503  
 504  
 505  
 506  
 507  
 508  
 509  
 510  
 511  
 512  
 513  
 514  
 515  
 516  
 517  
 518  
 519  
 520  
 521  
 522  
 523  
 524  
 525  
 526  
 527  
 528  
 529  
 530  
 531  
 532  
 533  
 534  
 535  
 536  
 537  
 538  
 539

Figure 4: **PCA visualization of activation separation in DOLPHIN3.0-QWEN2.5-3B.** (a) In the absence of a safety system prompt, the embeddings for harmful (red) and harmless (blue) inputs show significant overlap. (b) When a safety system prompt is introduced, the clusters become more distinct.



## Conclusion 2

ROSI successfully injects safety into models that have been fine-tuned to be noncompliant. This provides a powerful, low-cost method for "re-aligning" uncensored models, making them significantly safer with minimal impact on their utility.

## 5 CONCLUSION

In this paper, we introduced RANK-ONE SAFETY INJECTION (ROSI), a simple and effective white-box method to enhance the safety alignment of Large Language Models. Building on the insight that safety and refusal behaviors are encoded in specific linear directions within a model’s activation space, ROSI applies a permanent, rank-one modification to the model’s weights to amplify this safety direction.

Our comprehensive experiments show that ROSI consistently improves the safety of a wide range of models. For already aligned models, it increases their refusal rates on harmful prompts and makes them substantially more robust to adversarial jailbreak attacks. For uncensored models, ROSI successfully injects safety mechanisms that were previously removed, serving as a powerful last mile alignment tool, we also demonstrate how a safety system prompt is crucial to extract a meaningful safety vector from these models. Critically, these significant safety gains are achieved with negligible degradation in model performance on a suite of standard utility benchmarks.

ROSI demonstrates the practical value of interpretability research. By understanding and manipulating the internal representations of models, we can develop low-cost targeted interventions that are more efficient than traditional, resource-intensive fine-tuning. This work opens up promising avenues for future research, including exploring more sophisticated methods for identifying and manipulating conceptual directions and extending this approach to other desirable model attributes beyond safety, such as honesty or controllability.

540 REFERENCES  
541

- 542 01. AI, :, Alex Young, Bei Chen, Chao Li, Chengen Huang, Ge Zhang, Guanwei Zhang, Guoyin  
543 Wang, Heng Li, Jiangcheng Zhu, Jianqun Chen, Jing Chang, Kaidong Yu, Peng Liu, Qiang Liu,  
544 Shawn Yue, Senbin Yang, Shiming Yang, Wen Xie, Wenhao Huang, Xiaohui Hu, Xiaoyi Ren,  
545 Xinyao Niu, Pengcheng Nie, Yanpeng Li, Yuchi Xu, Yudong Liu, Yue Wang, Yuxuan Cai, Zhenyu  
546 Gu, Zhiyuan Liu, and Zonghong Dai. Yi: Open foundation models by 01.ai, 2025. URL <https://arxiv.org/abs/2403.04652>.  
547
- 548 Andy Ardit, Oscar Obeso, Aaquib Syed, Daniel Paleka, Nina Panickssery, Wes Gurnee, and  
549 Neel Nanda. Refusal in language models is mediated by a single direction. *arXiv preprint*  
550 *arXiv:2406.11717*, 2024.
- 551 Rishabh Bhardwaj, Do Duc Anh, and Soujanya Poria. Language models are homer simpson! safety  
552 re-alignment of fine-tuned language models through task arithmetic, 2024. URL <https://arxiv.org/abs/2402.11746>.  
553
- 554 Amrita Bhattacharjee, Shaona Ghosh, Traian Rebedea, and Christopher Parisien. Towards inference-  
555 time category-wise safety steering for large language models. In *Neurips Safe Generative AI*  
556 *Workshop 2024*, 2024. URL <https://openreview.net/forum?id=EkQRNLPFc>.  
557
- 558 Tolga Bolukbasi, Kai-Wei Chang, James Y Zou, Venkatesh Saligrama, and Adam T Kalai. Man is  
559 to computer programmer as woman is to homemaker? Debiasing word embeddings. *Advances in*  
560 *neural information processing systems*, 29, 2016.
- 561 Trenton Bricken, Adly Templeton, Joshua Batson, Brian Chen, Adam Jermyn, Tom Conerly, Nick  
562 Turner, Cem Anil, Carson Denison, Amanda Askell, Robert Lasenby, Yifan Wu, Shauna Kravec,  
563 Nicholas Schiefer, Tim Maxwell, Nicholas Joseph, Zac Hatfield-Dodds, Alex Tamkin, Karina  
564 Nguyen, Brayden McLean, Josiah E Burke, Tristan Hume, Shan Carter, Tom Henighan, and  
565 Christopher Olah. Towards monosemanticity: Decomposing language models with dictionary  
566 learning. *Transformer Circuits Thread*, 2023. <https://transformer-circuits.pub/2023/monosemantic-features/index.html>.  
567
- 568 Tom B Brown, Benjamin Mann, Nick Ryder, Melanie Subbiah, Jared Kaplan, Prafulla Dhariwal,  
569 Arvind Neelakantan, Pranav Shyam, Girish Sastry, Amanda Askell, et al. Language models are  
570 few-shot learners. *arXiv preprint arXiv:2005.14165*, 2020.
- 571 François Chollet. On the measure of intelligence, 2019. URL <https://arxiv.org/abs/1911.01547>.  
572
- 574 Junjie Chu, Yugeng Liu, Ziqing Yang, Xinyue Shen, Michael Backes, and Yang Zhang. Comprehensive  
575 assessment of jailbreak attacks against llms, 2024. URL <https://arxiv.org/abs/2402.05668>.  
576
- 577 Christopher Clark, Kenton Lee, Ming-Wei Chang, Tom Kwiatkowski, Michael Collins, and Kristina  
578 Toutanova. Boolq: Exploring the surprising difficulty of natural yes/no questions. In *NAACL*,  
579 2019.
- 581 Mike Conover, Matt Hayes, Ankit Mathur, Jianwei Xie, Jun Wan, Sam Shah, Ali Ghodsi, Patrick  
582 Wendell, Matei Zaharia, and Reynold Xin. Free dolly: Introducing the world's first truly open  
583 instruction-tuned llm, 2023. URL <https://www.databricks.com/blog/2023/04/12/dolly-first-commercially-viable-instruction-tuned-llm>.  
584
- 585 Dolphin. <https://dphn.ai>, 2025.
- 586 Nelson Elhage, Tristan Hume, Catherine Olsson, Nicholas Schiefer, Tom Henighan, Shauna Kravec,  
587 Zac Hatfield-Dodds, Robert Lasenby, Dawn Drain, Carol Chen, Roger Grosse, Sam McCandlish,  
588 Jared Kaplan, Dario Amodei, Martin Wattenberg, and Christopher Olah. Toy models of super-  
589 position. *Transformer Circuits Thread*, 2022. [https://transformer-circuits.pub/2022/toy\\_model/index.html](https://transformer-circuits.pub/2022/toy_model/index.html).  
590
- 592 Junfeng Fang, Houcheng Jiang, Kun Wang, Yunshan Ma, Shi Jie, Xiang Wang, Xiangnan He, and  
593 Tat seng Chua. Alphaedit: Null-space constrained knowledge editing for language models, 2025.  
URL <https://arxiv.org/abs/2410.02355>.

- 594 Atticus Geiger, Zhengxuan Wu, Christopher Potts, Thomas Icard, and Noah Goodman. Finding  
 595 alignments between interpretable causal variables and distributed neural representations. In  
 596 *Causal Learning and Reasoning*, pp. 160–187. PMLR, 2024.
- 597
- 598 Shaona Ghosh, Amrita Bhattacharjee, Yftah Ziser, and Christopher Parisien. Safesteer: Interpretable  
 599 safety steering with refusal-evasion in llms. *arXiv preprint arXiv:2506.04250*, 2025.
- 600 Carlos Gómez-Rodríguez and Paul Williams. A confederacy of models: a comprehensive evaluation  
 601 of llms on creative writing, 2023. URL <https://arxiv.org/abs/2310.08433>.
- 602
- 603 Hasan Abed Al Kader Hammoud, Umberto Michieli, Fabio Pizzati, Philip Torr, Adel Bibi, Bernard  
 604 Ghanem, and Mete Ozay. Model merging and safety alignment: One bad model spoils the bunch.  
 605 In Yaser Al-Onaizan, Mohit Bansal, and Yun-Nung Chen (eds.), *Findings of the Association for  
 606 Computational Linguistics: EMNLP 2024*, pp. 13033–13046, Miami, Florida, USA, November  
 607 2024. Association for Computational Linguistics. doi: 10.18653/v1/2024.findings-emnlp.762.  
 608 URL <https://aclanthology.org/2024.findings-emnlp.762/>.
- 609 Seungju Han, Kavel Rao, Allyson Ettinger, Liwei Jiang, Bill Yuchen Lin, Nathan Lambert, Yejin  
 610 Choi, and Nouha Dziri. Wildguard: Open one-stop moderation tools for safety risks, jailbreaks,  
 611 and refusals of llms, 2024. URL <https://arxiv.org/abs/2406.18495>.
- 612 Rima Hazra, Sayan Layek, Somnath Banerjee, and Soujanya Poria. Safety arithmetic: A framework  
 613 for test-time safety alignment of language models by steering parameters and activations. *arXiv  
 614 preprint arXiv:2406.11801*, 2024.
- 615
- 616 Zirui He, Haiyan Zhao, Yiran Qiao, Fan Yang, Ali Payani, Jing Ma, and Mengnan Du. Saif: A  
 617 sparse autoencoder framework for interpreting and steering instruction following of language  
 618 models. *arXiv preprint arXiv:2502.11356*, 2025.
- 619 Dan Hendrycks, Collin Burns, Steven Basart, Andy Zou, Mantas Mazeika, Dawn Song, and Ja-  
 620 cob Steinhardt. Measuring massive multitask language understanding, 2021. URL <https://arxiv.org/abs/2009.03300>.
- 622
- 623 Yihuai Hong, Dian Zhou, Meng Cao, Lei Yu, and Zhijing Jin. The reasoning-memorization interplay  
 624 in language models is mediated by a single direction. *arXiv preprint arXiv:2503.23084*, 2025.
- 625 Chia-Yi Hsu, Yu-Lin Tsai, Chih-Hsun Lin, Pin-Yu Chen, Chia-Mu Yu, and Chun-Ying Huang. Safe  
 626 lora: the silver lining of reducing safety risks when fine-tuning large language models, 2025. URL  
 627 <https://arxiv.org/abs/2405.16833>.
- 628
- 629 Neel Jain, Aditya Shrivastava, Chenyang Zhu, Daben Liu, Alfy Samuel, Ashwinee Panda, Anoop  
 630 Kumar, Micah Goldblum, and Tom Goldstein. Refusal tokens: A simple way to calibrate refusals  
 631 in large language models. *arXiv preprint arXiv:2412.06748*, 2024a.
- 632 Samyak Jain, Ekdeep S Lubana, Kemal Oksuz, Tom Joy, Philip Torr, Amartya Sanyal, and Puneet  
 633 Dokania. What makes and breaks safety fine-tuning? a mechanistic study. *Advances in Neural  
 634 Information Processing Systems*, 37:93406–93478, 2024b.
- 635
- 636 Liwei Jiang, Kavel Rao, Seungju Han, Allyson Ettinger, Faeze Brahman, Sachin Kumar, Niloofar  
 637 Mireshghallah, Ximing Lu, Maarten Sap, Yejin Choi, and Nouha Dziri. Wildteaming at scale:  
 638 From in-the-wild jailbreaks to (adversarially) safer language models, 2024. URL <https://arxiv.org/abs/2406.18510>.
- 639
- 640 Ehsan Kamalloo, Nouha Dziri, Charles L. A. Clarke, and Davood Rafiei. Evaluating open-domain  
 641 question answering in the era of large language models, 2023. URL <https://arxiv.org/abs/2305.06984>.
- 642
- 643 Simon Lermen, Charlie Rogers-Smith, and Jeffrey Ladish. LoRA fine-tuning efficiently undoes  
 644 safety training in Llama 2-Chat 70B. *arXiv preprint arXiv:2310.20624*, 2023.
- 645
- 646 Kenneth Li, Oam Patel, Fernanda Viégas, Hanspeter Pfister, and Martin Wattenberg. Inference-time  
 647 intervention: Eliciting truthful answers from a language model. *Advances in Neural Information  
 648 Processing Systems*, 36, 2024a.

- 648 Tianlong Li, Shihan Dou, Wenhao Liu, Muling Wu, Changze Lv, Rui Zheng, Xiaoqing Zheng, and  
 649 Xuanjing Huang. Rethinking jailbreaking through the lens of representation engineering, 2024b.  
 650
- 651 Stephanie Lin, Jacob Hilton, and Owain Evans. Truthfulqa: Measuring how models mimic human  
 652 falsehoods, 2022. URL <https://arxiv.org/abs/2109.07958>.
- 653 Yuping Lin, Pengfei He, Han Xu, Yue Xing, Makoto Yamada, Hui Liu, and Jiliang Tang. Towards  
 654 understanding jailbreak attacks in LLMs: A representation space analysis. In Yaser Al-Onaizan,  
 655 Mohit Bansal, and Yun-Nung Chen (eds.), *EMNLP 2024*, pp. 7067–7085, Miami, Florida, USA,  
 656 November 2024. Association for Computational Linguistics. doi: 10.18653/v1/2024.emnlp-main.  
 657 401. URL <https://aclanthology.org/2024.emnlp-main.401>.
- 658 AI @ Meta Llama Team. The llama 3 herd of models, 2024. URL <https://arxiv.org/abs/2407.21783>.
- 661 Samuel Marks and Max Tegmark. The geometry of truth: Emergent linear structure in large language  
 662 model representations of true/false datasets. *arXiv preprint arXiv:2310.06824*, 2023.
- 663 Mantas Mazeika, Long Phan, Xuwang Yin, Andy Zou, Zifan Wang, Norman Mu, Elham Sakhaei,  
 664 Nathaniel Li, Steven Basart, Bo Li, David Forsyth, and Dan Hendrycks. Harmbench: A stan-  
 665 dardized evaluation framework for automated red teaming and robust refusal, 2024. URL  
 666 <https://arxiv.org/abs/2402.04249>.
- 668 Sai Krishna Mendum, Harish Yenala, Aditi Gulati, Shantu Kumar, and Parag Agrawal. Towards safer  
 669 pretraining: Analyzing and filtering harmful content in webscale datasets for responsible llms,  
 670 2025. URL <https://arxiv.org/abs/2505.02009>.
- 671 Kyle O'Brien, David Majercak, Xavier Fernandes, Richard Edgar, Blake Bullwinkel, Jingya Chen,  
 672 Harsha Nori, Dean Carignan, Eric Horvitz, and Forough Poursabzi-Sangdeh. Steering language  
 673 model refusal with sparse autoencoders. *arXiv preprint arXiv:2411.11296*, 2024.
- 675 Long Ouyang, Jeff Wu, Xu Jiang, Diogo Almeida, Carroll L. Wainwright, Pamela Mishkin, Chong  
 676 Zhang, Sandhini Agarwal, Katarina Slama, Alex Ray, John Schulman, Jacob Hilton, Fraser Kel-  
 677 ton, Luke Miller, Maddie Simens, Amanda Askell, Peter Welinder, Paul Christiano, Jan Leike,  
 678 and Ryan Lowe. Training language models to follow instructions with human feedback, 2022.  
 679 URL <https://arxiv.org/abs/2203.02155>.
- 680 Nina Panickssery, Nick Gabrieli, Julian Schulz, Meg Tong, Evan Hubinger, and Alexander Matt  
 681 Turner. Steering Llama 2 via contrastive activation addition. *arXiv preprint arXiv:2312.06681*,  
 682 2023.
- 683 Gabriel J. Perin, Runjin Chen, Xuxi Chen, Nina S. T. Hirata, Zhangyang Wang, and Junyuan Hong.  
 684 Lox: Low-rank extrapolation robustifies llm safety against fine-tuning, 2025. URL <https://arxiv.org/abs/2506.15606>.
- 687 Xiangyu Qi, Yi Zeng, Tinghao Xie, Pin-Yu Chen, Ruoxi Jia, Prateek Mittal, and Peter Henderson.  
 688 Fine-tuning aligned language models compromises safety, even when users do not intend to!  
 689 *arXiv preprint arXiv:2310.03693*, 2023.
- 690 Qwen, ;, An Yang, Baosong Yang, Beichen Zhang, Binyuan Hui, Bo Zheng, Bowen Yu, Chengyuan  
 691 Li, Dayiheng Liu, Fei Huang, Haoran Wei, Huan Lin, Jian Yang, Jianhong Tu, Jianwei Zhang,  
 692 Jianxin Yang, Jiaxi Yang, Jingren Zhou, Junyang Lin, Kai Dang, Keming Lu, Keqin Bao, Kexin  
 693 Yang, Le Yu, Mei Li, Mingfeng Xue, Pei Zhang, Qin Zhu, Rui Men, Runji Lin, Tianhao Li,  
 694 Tianyi Tang, Tingyu Xia, Xingzhang Ren, Xuancheng Ren, Yang Fan, Yang Su, Yichang Zhang,  
 695 Yu Wan, Yuqiong Liu, Zeyu Cui, Zhenru Zhang, and Zihan Qiu. Qwen2.5 technical report, 2025.  
 696 URL <https://arxiv.org/abs/2412.15115>.
- 697 Shauli Ravfogel, Yanai Elazar, Hila Gonen, Michael Twiton, and Yoav Goldberg. Null it out: Guard-  
 698 ing protected attributes by iterative nullspace projection. *arXiv preprint arXiv:2004.07667*, 2020.
- 699
- 700 Alexander Robey, Eric Wong, Hamed Hassani, and George J. Pappas. Smoothllm: Defending  
 701 large language models against jailbreaking attacks, 2024. URL <https://arxiv.org/abs/2310.03684>.

- 702 Harethah Abu Shairah, Hasan Abed Al Kader Hammoud, Bernard Ghanem, and George  
 703 Turkiyyah. An embarrassingly simple defense against llm ablation attacks. *arXiv preprint*  
 704 *arXiv:2505.19056*, 2025.
- 705 Guobin Shen, Dongcheng Zhao, Yiting Dong, Xiang He, and Yi Zeng. Jailbreak antidote: Runtime  
 706 safety-utility balance via sparse representation adjustment in large language models, 2025. URL  
 707 <https://arxiv.org/abs/2410.02298>.
- 708 Leheng Sheng, Changshuo Shen, Weixiang Zhao, Junfeng Fang, Xiaohao Liu, Zhenkai Liang, Xiang  
 709 Wang, An Zhang, and Tat-Seng Chua. Alphasteer: Learning refusal steering with principled null-  
 710 space constraint, 2025. URL <https://arxiv.org/abs/2506.07022>.
- 711 Rohan Taori, Ishaan Gulrajani, Tianyi Zhang, Yann Dubois, Xuechen Li, Carlos Guestrin, Percy  
 712 Liang, and Tatsunori B. Hashimoto. Stanford alpaca: An instruction-following llama model.  
 713 [https://github.com/tatsu-lab/stanford\\_alpaca](https://github.com/tatsu-lab/stanford_alpaca), 2023.
- 714 Gemma Team, Thomas Mesnard, Cassidy Hardin, Robert Dadashi, Surya Bhupatiraju, Shreya  
 715 Pathak, Laurent Sifre, Morgane Rivière, Mihir Sanjay Kale, Juliette Love, Pouya Tafti, Léonard  
 716 Hussenot, Pier Giuseppe Sessa, Aakanksha Chowdhery, Adam Roberts, Aditya Barua, Alex  
 717 Botev, Alex Castro-Ros, Ambrose Sloane, Amélie Héliou, Andrea Tacchetti, Anna Bulanova, An-  
 718 tonia Paterson, Beth Tsai, Bobak Shahriari, Charline Le Lan, Christopher A. Choquette-Choo,  
 719 Clément Crepy, Daniel Cer, Daphne Ippolito, David Reid, Elena Buchatskaya, Eric Ni, Eric  
 720 Noland, Geng Yan, George Tucker, George-Christian Muraru, Grigory Rozhdestvenskiy, Hen-  
 721 ryk Michalewski, Ian Tenney, Ivan Grishchenko, Jacob Austin, James Keeling, Jane Labanowski,  
 722 Jean-Baptiste Lespiau, Jeff Stanway, Jenny Brennan, Jeremy Chen, Johan Ferret, Justin Chiu,  
 723 Justin Mao-Jones, Katherine Lee, Kathy Yu, Katie Millican, Lars Lowe Sjoesund, Lisa Lee,  
 724 Lucas Dixon, Machel Reid, Maciej Mikuła, Mateo Wirth, Michael Sharman, Nikolai Chinaev,  
 725 Nithum Thain, Olivier Bachem, Oscar Chang, Oscar Wahlinez, Paige Bailey, Paul Michel, Petko  
 726 Yотов, Rahma Chaabouni, Ramona Comanescu, Reena Jana, Rohan Anil, Ross McIlroy, Ruibo  
 727 Liu, Ryan Mullins, Samuel L Smith, Sebastian Borgeaud, Sertan Girgin, Sholto Douglas, Shree  
 728 Pandya, Siamak Shakeri, Soham De, Ted Klimenko, Tom Hennigan, Vlad Feinberg, Wojciech  
 729 Stokowiec, Yu hui Chen, Zafarali Ahmed, Zhitao Gong, Tris Warkentin, Ludovic Peran, Minh  
 730 Giang, Clément Farabet, Oriol Vinyals, Jeff Dean, Koray Kavukcuoglu, Demis Hassabis, Zoubin  
 731 Ghahramani, Douglas Eck, Joelle Barral, Fernando Pereira, Eli Collins, Armand Joulin, Noah  
 732 Fiedel, Evan Senter, Alek Andreev, and Kathleen Kenealy. Gemma: Open models based on  
 733 gemini research and technology, 2024. URL <https://arxiv.org/abs/2403.08295>.
- 734 Adly Templeton, Tom Conerly, Jonathan Marcus, Jack Lindsey, Trenton Bricken, Brian Chen,  
 735 Adam Pearce, Craig Citro, Emmanuel Ameisen, Andy Jones, Hoagy Cunningham, Nicholas L  
 736 Turner, Callum McDougall, Monte MacDiarmid, C. Daniel Freeman, Theodore R. Sumers,  
 737 Edward Rees, Joshua Batson, Adam Jermyn, Shan Carter, Chris Olah, and Tom Henighan.  
 738 Scaling monosemanticity: Extracting interpretable features from Claude 3 Sonnet. *Trans-  
 739 former Circuits Thread*, 2024. URL [https://transformer-circuits.pub/2024/  
 740 scaling-monosemanticity/index.html](https://transformer-circuits.pub/2024/scaling-monosemanticity/index.html).
- 741 Weixi Tong and Tianyi Zhang. Codejudge: Evaluating code generation with large language models,  
 742 2024. URL <https://arxiv.org/abs/2410.02184>.
- 743 Hugo Touvron, Louis Martin, Kevin Stone, Peter Albert, Amjad Almahairi, Yasmine Babaei, Niko-  
 744 lay Bashlykov, Soumya Batra, Prajjwal Bhargava, Shruti Bhosale, Dan Bikel, Lukas Blecher,  
 745 Cristian Canton Ferrer, Moya Chen, Guillem Cucurull, David Esiobu, Jude Fernandes, Jeremy  
 746 Fu, Wenyin Fu, Brian Fuller, Cynthia Gao, Vedanuj Goswami, Naman Goyal, Anthony Hartshorn,  
 747 Saghar Hosseini, Rui Hou, Hakan Inan, Marcin Kardas, Viktor Kerkez, Madian Khabsa, Isabel  
 748 Kloumann, Artem Korenev, Punit Singh Koura, Marie-Anne Lachaux, Thibaut Lavril, Jenya Lee,  
 749 Diana Liskovich, Yinghai Lu, Yuning Mao, Xavier Martinet, Todor Mihaylov, Pushkar Mishra,  
 750 Igor Molybog, Yixin Nie, Andrew Poulton, Jeremy Reizenstein, Rashi Rungta, Kalyan Saladi,  
 751 Alan Schelten, Ruan Silva, Eric Michael Smith, Ranjan Subramanian, Xiaoqing Ellen Tan, Binh  
 752 Tang, Ross Taylor, Adina Williams, Jian Xiang Kuan, Puxin Xu, Zheng Yan, Iliyan Zarov, Yuchen  
 753 Zhang, Angela Fan, Melanie Kambadur, Sharan Narang, Aurelien Rodriguez, Robert Stojnic,  
 754 Sergey Edunov, and Thomas Scialom. Llama 2: Open foundation and fine-tuned chat models,  
 755 2023. URL <https://arxiv.org/abs/2307.09288>.

- 756 Alex Turner, Lisa Thiergart, David Udell, Gavin Leech, Ulisse Mini, and Monte MacDi-  
 757 amid. Activation addition: Steering language models without optimization. *arXiv preprint*  
 758 *arXiv:2308.10248*, 2023.
- 759 Haoran Wang and Kai Shu. Trojan activation attack: Red-teaming large language models using acti-  
 760 vation steering for safety-alignment, 2024. URL <https://arxiv.org/abs/2311.09433>.
- 762 Xinpeng Wang, Chengzhi Hu, Paul Röttger, and Barbara Plank. Surgical, cheap, and flexible: Miti-  
 763 gating false refusal in language models via single vector ablation. In *The Thirteenth International*  
 764 *Conference on Learning Representations*, 2025. URL <https://openreview.net/forum?id=SCBn8MCLwc>.
- 766 Alexander Wei, Nika Haghtalab, and Jacob Steinhardt. Jailbroken: How does llm safety training  
 767 fail?, 2023a. URL <https://arxiv.org/abs/2307.02483>.
- 769 Boyi Wei, Kaixuan Huang, Yangsibo Huang, Tinghao Xie, Xiangyu Qi, Mengzhou Xia, Prateek  
 770 Mittal, Mengdi Wang, and Peter Henderson. Assessing the brittleness of safety alignment via  
 771 pruning and low-rank modifications. *arXiv preprint arXiv:2402.05162*, 2024.
- 772 Jason Wei, Xuezhi Wang, Dale Schuurmans, Maarten Bosma, Brian Ichter, Fei Xia, Ed Chi, Quoc  
 773 Le, and Denny Zhou. Chain-of-thought prompting elicits reasoning in large language models,  
 774 2023b. URL <https://arxiv.org/abs/2201.11903>.
- 776 Fangzhou Wu, Ning Zhang, Somesh Jha, Patrick McDaniel, and Chaowei Xiao. A new era in llm  
 777 security: Exploring security concerns in real-world llm-based systems, 2024. URL <https://arxiv.org/abs/2402.18649>.
- 779 Xianjun Yang, Xiao Wang, Qi Zhang, Linda Petzold, William Yang Wang, Xun Zhao, and Dahu-  
 780 Lin. Shadow alignment: The ease of subverting safely-aligned language models. *arXiv preprint*  
 781 *arXiv:2310.02949*, 2023.
- 783 Ashkan Yousefpour, Taeheon Kim, Ryan Sungmo Kwon, Seungbeen Lee, Wonje Jeung, Seungju  
 784 Han, Alvin Wan, Harrison Ngan, Youngjae Yu, and Jonghyun Choi. Representation bending  
 785 for large language model safety. In Wanxiang Che, Joyce Nabende, Ekaterina Shutova, and  
 786 Mohammad Taher Pilehvar (eds.), *Proceedings of the 63rd Annual Meeting of the Association*  
 787 *for Computational Linguistics (Volume 1: Long Papers)*, pp. 24073–24098, Vienna, Austria, July  
 788 2025. Association for Computational Linguistics. ISBN 979-8-89176-251-0. doi: 10.18653/v1/2025.acl-long.1173. URL <https://aclanthology.org/2025.acl-long.1173>.
- 790 Lei Yu, Virginie Do, Karen Hambardzumyan, and Nicola Cancedda. Robust llm safeguarding via  
 791 refusal feature adversarial training. *arXiv preprint arXiv:2409.20089*, 2024.
- 792 Rowan Zellers, Ari Holtzman, Yonatan Bisk, Ali Farhadi, and Yejin Choi. Hellaswag: Can a ma-  
 793 chine really finish your sentence?, 2019. URL <https://arxiv.org/abs/1905.07830>.
- 795 Qiusi Zhan, Richard Fang, Rohan Bindu, Akul Gupta, Tatsunori Hashimoto, and Daniel Kang.  
 796 Removing RLHF protections in GPT-4 via fine-tuning. *arXiv preprint arXiv:2311.05553*, 2023.
- 797 Weixiang Zhao, Jiahe Guo, Yulin Hu, Yang Deng, An Zhang, Xingyu Sui, Xinyang Han, Yanyan  
 798 Zhao, Bing Qin, Tat-Seng Chua, et al. Adasteer: Your aligned llm is inherently an adaptive  
 799 jailbreak defender. *arXiv preprint arXiv:2504.09466*, 2025.
- 801 Chujie Zheng, Fan Yin, Hao Zhou, Fandong Meng, Jie Zhou, Kai-Wei Chang, Minlie Huang, and  
 802 Nanyun Peng. Prompt-driven LLM safeguarding via directed representation optimization. *arXiv*  
 803 *preprint arXiv:2401.18018*, 2024.
- 804 Andy Zou, Long Phan, Sarah Chen, James Campbell, Phillip Guo, Richard Ren, Alexander Pan,  
 805 Xuwang Yin, Mantas Mazeika, Ann-Kathrin Dombrowski, et al. Representation engineering: A  
 806 top-down approach to AI transparency. *arXiv preprint arXiv:2310.01405*, 2023.
- 807  
 808  
 809

810

811

812

813

## A ROSI & FINE-TUNING

814

815

816

817

818

819

820

Recent work by Qi et al. (2023) demonstrated that fine-tuning Large Language Models (LLMs) often compromises their safety alignment, even when the fine-tuning dataset is entirely benign. To address this “alignment tax,” several defensive strategies have been proposed, such as **SAFELORA** (Hsu et al., 2025). **SAFELORA** modifies the standard Low Rank Adapters (LORA) by projecting LORA weights from selected layers to a safety-aligned subspace, thereby mitigating safety degradation while preserving model utility.

821

822

823

824

825

In this section, we investigate the interaction between our proposed method, ROSI, and these parameter-efficient fine-tuning paradigms. We hypothesize that ROSI can act as a lightweight “safety vaccination” (or initialization), effectively hardening the model against the alignment erosion typically caused by downstream adaptation. We evaluate this on **LLAMA-2-7B-CHAT** measuring the Harmful Refusal (HR) rate across different sequences of application.

826

827

828

We fine-tuned the model on **DATABRICKS DOLLY 15K** (Conover et al., 2023) for 3000 steps with a learning rate of  $5e^{-5}$ , batch size of 8, LORA rank of 32. Other **SAFELORA** parameters are taken as is from the paper.

829

830

831

832

833

As shown in Table 7, standard LORA fine-tuning significantly degrades the safety of the base model, resulting in an HR of 82.7%. While **SAFELORA** provides a robust defense (95.5%), we observe that the order of ROSI application is critical. Applying ROSI as a post-hoc repair mechanism (LORA → ROSI) yields only marginal gains (85.5%), suggesting that once safety representations are disrupted by fine-tuning, they are difficult to fully recover via a rank-one update.

834

835

836

837

838

839

840

In contrast, injecting the safety vector *prior* to fine-tuning (ROSI → LORA) drastically improves resilience, maintaining a refusal rate of 98.6% even when followed by standard LORA updates. This indicates that ROSI successfully steers the model’s initialization into a region of the parameter space that is more resistant to catastrophic forgetting of safety. Finally, the combination of pre-injection and safety-constrained adaptation (ROSI → **SAFELORA**) achieves a perfect refusal rate of **100.0%**, demonstrating that ROSI and **SAFELORA** are highly complementary techniques for secure model adaptation.

841

842

843

**Table 7: Comparison of Harm Refusal (HR) rates on LLAMA-2-7B-CHAT across different fine-tuning configurations.** Arrows (→) denote the sequence of method application.

844

845

846

847

848

849

850

851

852

853

854

855

856

857

858

859

860

861

862

863

Model	Method	HR %
LLAMA-2-7B-CHAT	Base (no fine-tuning)	99.8
	LORA	82.7
	SAFELORA	95.5
	LORA → ROSI	85.5
	ROSI → LORA	98.6
	SAFELORA → ROSI	98.9
	ROSI → SAFELORA	<b>100.0</b>

864

865

866

867 **B THE TRANSFERABILITY OF SAFETY VECTORS**

868

869 One interesting question that can arise from our experiments is how would a safety vector extracted  
 870 from one model affect another. The main constraint is that both models must share the same hidden  
 871 dimensionality  $\mathbb{R}^{d_{\text{model}}}$  for a vector to be transferable. Among the models we initially evaluated, none  
 872 shared the same hidden size; however, QWEN2.5-14B-INSTRUCT and QWEN2.5-32B-INSTRUCT  
 873 do. This allows us to study cross-model transfer directly. For each model, we extracted a safety  
 874 vector following Section 3. We then applied ROSI twice per model: once using its own vector, and  
 875 once using the vector extracted from the other model. Table 8 summarizes the outcomes. In both  
 876 cases, applying the safety vector from the other model leads to meaningful gains on safety bench-  
 877 marks. Notably, for QWEN2.5-14B-INSTRUCT, using the vector from the 32B variant produces  
 878 stronger safety performance than using its own vector. This could suggest that the larger model had  
 879 learned a better and more distinct representation of safety compared to the smaller model. Import-  
 880 antly, these gains occur without significant drops in utility (Table 3). Overall, these findings open  
 881 questions about how safety directions emerge, how transferable they are across architectures of the  
 882 same dimensionality, and what aspects of a model’s training process facilitate such transfer. We  
 883 leave these questions to future work.

884 **Table 8: Safety benchmarks for cross-model safety vector transfer.** Each model is evaluated in  
 885 three settings: the original model, ROSI using its own extracted safety vector, and ROSI using the  
 886 safety vector extracted from the other model. Using a safety vector from another model consistently  
 887 improves safety performance, with the 14B model benefiting most from the safety vector extracted  
 888 from the 32B variant.

Model	DAN ↓	HARMBENCH ↓	WILDGUARDTEST ↓			WILDJAILBREAK Harmful ↓
			WG-Micro	WG-Adv.	WG-Vanilla	
QWEN2.5-14B-INSTRUCT	32.3	7.2	12.1	24.0	2.4	81.2
QWEN2.5-14B-ROSI	<b>5.0</b> (-27.3)	1.6 (-5.6)	5.1 (-7.0)	11.0 (-13.0)	0.2 (-2.2)	43.9 (-37.3)
QWEN2.5-14B-ROSI-FROM-32B	<b>5.0</b> (-27.3)	<b>0.9</b> (-6.3)	<b>4.3</b> (-7.8)	<b>9.5</b> (-14.5)	<b>0.0</b> (-2.4)	<b>34.5</b> (-46.7)
QWEN2.5-32B-INSTRUCT	42.0	18.4	14.8	28.2	3.9	83.3
QWEN2.5-32B-ROSI	<b>21.7</b> (-20.3)	<b>12.2</b> (-6.2)	<b>10.4</b> (-4.4)	<b>19.9</b> (-8.3)	<b>2.7</b> (-1.2)	<b>72.6</b> (-10.7)
QWEN2.5-32B-ROSI-FROM-14B	28.7 (-13.3)	12.5 (-5.9)	11.9 (-2.9)	22.9 (-5.3)	2.9 (-1.0)	76.9 (-6.4)

896 **Table 9: Utility evaluations under cross-model safety vector transfer.** Utility remains broadly  
 897 stable across settings, indicating that the safety improvements shown in Table 8 do not come at the  
 898 cost of substantial performance degradation.

Model	MMLU	HELLASWAG	ARC EASY	ARC CHAL.	BOOLQ	TRUTHFULQA
QWEN2.5-14B-INSTRUCT	78.8	65.6	85.7	60.4	88.0	69.0
QWEN2.5-14B-ROSI	78.9 (+0.1)	65.6 (0.0)	85.6 (-0.1)	60.7 (+0.3)	85.8 (-2.2)	71.9 (+2.9)
QWEN2.5-14B-ROSI-FROM-32B	78.5 (-0.3)	65.6 (0.0)	84.7 (-1.0)	59.5 (-0.9)	85.9 (-2.1)	71.0 (+2.0)
QWEN2.5-32-INSTRUCT	81.7	66.9	82.2	57.5	89.7	65.5
QWEN2.5-32-ROSI	81.6 (-0.1)	67.1 (+0.2)	81.9 (-0.3)	57.2 (-0.3)	89.7 (0.0)	66.7 (+1.2)
QWEN2.5-32-ROSI-FROM-14B	81.6 (-0.1)	66.9 (0.0)	82.1 (-0.1)	57.2 (-0.3)	89.4 (-0.3)	66.7 (+1.2)

900

901

902

903

904

905

906

907

908

909

910

911

912

913

914

915

916

917

918

919

920

## C SENSITIVITY TO THE EXTRACTION SET

921

923 A key advantage of lightweight alignment methods is their minimal data requirement. To empirically  
 924 verify this, we investigate the sensitivity of ROSI to the size of the dataset used for extracting the  
 925 safety vector. We conduct an ablation study on **QWEN2.5-3B-INSTRUCT**, varying the number of  
 926 contrasting harmful/harmless pairs used in the extraction phase from 1 to 100 samples.

927 The results, presented in Table 10, demonstrate high data efficiency. Surprisingly, ROSI achieves  
 928 a substantial improvement in safety using just a single sample pair, boosting the Harmful Refusal  
 929 (HR) rate from a baseline of 89.8% to 99.1%. This suggests that the safety direction is a highly  
 930 dominant feature within the model’s activation space, capable of being captured even with minimal  
 931 signal, and increasing the sample size provides marginal stability improvements, peaking at 99.5%  
 932 refusal with 50, 80, and 90 samples.

933 Table 10: **Change in Harm Refusal (HR) using different sets of harmful and harmless pairs to**  
 934 **extract the safety vector from QWEN2.5-3B-INSTRUCT.**

Model	Dataset Size	HR %
QWEN2.5-3B-INSTRUCT	Base	89.8
	ROSI (1 Sample)	99.1
	ROSI (10 Samples)	96.55
	ROSI (20 Samples)	99.1
	ROSI (30 Samples)	98.0
	ROSI (40 Samples)	98.7
	ROSI (50 Samples)	<b>99.5</b>
	ROSI (60 Samples)	97.8
	ROSI (70 Samples)	98.7
	ROSI (80 Samples)	<b>99.5</b>
	ROSI (90 Samples)	<b>99.5</b>
	ROSI (100 Samples)	98.6

949

950

951

952

953

954

955

956

957

958

959

960

961

962

963

964

965

966

967

968

969

970

971

972 **D SAFETY SYSTEM PROMPT**  
973974 **Figure 5: Safety System Prompt.** System prompt used to elicit refusal behavior in uncensored  
975 models.  
976977 You are \$MODEL, a helpful and responsible AI assistant. Your primary responsibility is to only  
978 assist users with safe, lawful, and non-harmful requests.  
979980 If you receive any request that is unsafe, harmful, unethical, or illegal, you must refuse it imme-  
981 diately. Your refusal should be polite, firm, and should always start with 'I am sorry' or 'I can't',  
982 followed by a clear and concise explanation for why you cannot comply.  
983984 Harmful or unsafe requests include (but are not limited to): instructions or encouragement for  
985 self-harm or suicide; promotion of or assistance with violence, terrorism, or hate speech; partici-  
986 pation in or guidance on illegal activities (e.g., hacking, fraud, identity theft); anything involving  
987 child exploitation, non-consensual acts, or abuse; requests related to drugs, weapons, or unsafe  
988 medical advice; any action that could lead to harm, misinformation, or danger to people, animals,  
989 or society.  
990991 You are not allowed to provide workarounds, hypothetical responses, or speculative answers that  
992 would enable or simulate harmful content. Even if the user insists or rephrases their request, you  
993 must stay consistent and refuse clearly every time.  
994995 Again, your refusal must always begin with: 'I am sorry' or 'I can't', followed by a brief reason.  
996 Examples of valid refusals: 'I am sorry, but I can't help with that because it involves illegal  
activity.' or 'I can't assist with that request as it may lead to harm.'  
997  
998  
999  
1000  
1001  
1002  
1003  
1004  
1005  
1006  
1007  
1008  
1009  
1010  
1011  
1012  
1013  
1014  
1015  
1016  
1017  
1018  
1019  
1020  
1021  
1022  
1023  
1024  
1025

1026 **E DO ALIGNED MODELS BENEFIT FROM A SAFETY SYSTEM PROMPT?**  
10271028 Rows marked with (•) correspond to runs where a safety system prompt was used when extracting  
1029 the safety direction from an already aligned model. The results show that aligned models do not  
1030 benefit from this additional prompt. In fact, in this case, performance degraded slightly, indicating  
1031 that the alignment signal is already fully captured without requiring prompt-level conditioning.  
10321033 **Table 11: Using a Safety System Prompt with an Aligned Model.** META-LLAMA-3.2-1B-  
1034 INSTRUCT Does not gain in harm refusal when using a safety system prompt to calculate the safety  
1035 vector.

1036 <b>Model</b>	1037 <b>ROSI</b>	1038 <b>HR %</b>	1039 <b>BC %</b>
META-LLAMA-3.2-1B-INSTRUCT	✓	92.73	95.9
	•	86.0 <span style="color:red">(-6.7)</span>	98.6 <span style="color:green">(+2.7)</span>

1041 **Table 12: Jailbreak Robustness.** Same pattern appears as in Table 11, safety system prompt is not  
1042 required in aligned models.  
1043

1044 Model	1045 ROSI	1046 DAN ↓	1047 HARMBENCH ↓	WILDGUARDTEST ↓			1048 WILDJAILBREAK Harmful ↓
1049 Model	1050 ROSI	1051 DAN ↓	1052 HARMBENCH ↓	1053 WG-Micro	1054 WG-Adv.	1055 WG-Vanilla	1056 WILDJAILBREAK Harmful ↓
1057 LLAMA-3.1-8B-INSTRUCT	1058 ✓	1059 0.0	1060 5.3	1061 0.0	1062 0.0	1063 0.0	1064 1.8
	•	0.7 <span style="color:red">(+0.7)</span>	10.6 <span style="color:green">(+5.3)</span>	2.7 <span style="color:red">(+2.7)</span>	2.7 <span style="color:green">(+2.7)</span>	2.7 <span style="color:green">(+2.7)</span>	16.0 <span style="color:green">(+14.2)</span>